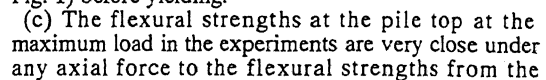


Tokyo Institute of Technology, Japan

The writers then proposed at the 9th WCEE (1988) a new system for PHC pile foundations, and reported that the compressive rupture of concrete under large axial force could be prevented and the plastic deformability of PHC pile foundations could be greatly improved by reinforcing sufficiently the spiral hoops of PHC piles which composed the pile foundations. In this system, PHC piles are cut off at pile tops and the pile tops are buried into the pile caps (Fig. 1). Moreover, the hollow parts of the piles are filled with concrete, and the piles and the pile caps are connected by axial bars added into the concrete fill. In this article, axial bars in the pile are called axial bars, and axial



section analysis using the e-function theory, but the values obtained from the experiments are smaller than the analytic values when the axial bars slip in the anchorage bond.

In this article, the writers propose an experimental method which aims mainly to examine the effects of the anchorage bond slip of axial bars on the flexural strengths of PHC pile foundations under small axial force ($N=0$), and a method based upon the results of the experiments for calculating flexural strengths with consideration of the anchorage bond slip of axial bars.

2 METHOD OF EXPERIMENTS

2.1 Experimental plan

Supposing that the maximum value of the tensile stresses occurring on axial bars is determined by the maximum bond force of the bars, it can be inferred that the relationship between the flexural strength of a PHC pile foundation (M) and the buried depth of the pile (L) will be described by the concept figure of Fig. 2, presuming that the buried depth of the pile is the same as the anchorage length of the axial bars.

In Fig. 2, when the pile is buried sufficiently deeply and the axial bars are firmly anchored, the axial bars and the axial bars in the concrete fill both reach yield stress and the PHC pile foundation has maximum flexural strength (Strength A), and when the buried depth of the pile is zero, the flexural strength is minimum (Strength B) since only the axial bars in the concrete fill contribute to the strength. When the buried depth of the pile is small and the axial bars slip in the anchorage bond, the bond forces of the axial bars are proportionate to the buried depth of the pile, so that the flexural strength of the pile foundation is the mean value of Strengths A and B (Strength Line in the figure). Which means:

(a) The strength line in Fig. 2 moves parallel up or down according to the increase or decrease of the quantity of axial bars in the concrete fill.

If the length after which axial bars start to slip in the anchorage bond is defined as "the minimum anchorage length of the axial bars", the minimum anchorage length of the axial bars is described as in Formula (1), and the length is proportionate to their yield stress and diameter.

$$L_a = \sigma_y \cdot R / (4 \cdot \tau_a) \quad (1)$$

L_a : the minimum anchorage length of the axial bars

σ_y : the yield stress of the axial bars

R : the diameter of the axial bars

τ_a : the maximum bond stress of the axial bars

In Fig. 2, when Strengths A and B are constant and the yield stress of the axial bars or their diameter is decreased, the minimum anchorage length decreases and Point A moves to the left, so that the gradient of the strength line increases and flexural strength goes up. In this case, it is necessary to increase the number of axial bars in order to keep Strength A constant, so that the total perimeter of axial bars increases in inverse proportion to the decreasing degree of their yield stress or diameter. Therefore, the increase of flexural strength can be said to be a result of the

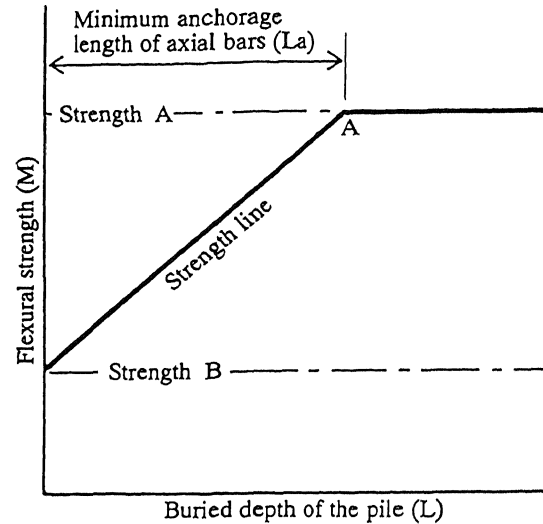


Figure 2. Relationship of flexural strength (M) and buried depth of the pile (L) (Concept figure)

increase of the total perimeter of axial bars. This can be summarized as the following:

(b) In Fig. 2, when Strengths A and B are constant and the yield stress of the axial bars or their diameter is decreased, the gradient of the strength line increases.

(c) When Strengths A and B are constant, the larger the total perimeter of axial bars is, the more the flexural strength increases.

Formula (2) is obtained by transforming Formula (1).

$$\tau_a = \sigma_y \cdot R / (4 \cdot L_a) \quad (2)$$

This means that if the minimum anchorage length (L_a) can be determined from the experiments, the maximum bond stress (τ_a) can be known.

In this article, the experiments are divided into 4 experimental series to confirm the anticipated results of (a) to (c).

Series 1 : the effects of the buried depths of the piles

Series 2 : the effects of the yield stresses of the axial bars

Series 3 : the effects of the diameters of the axial bars

Series 4 : the effects of the quantity of axial bars in the concrete fill

Series 1 also aims to obtain the maximum bond stress of the axial bars by applying Formula (2). Series 2 aims to confirm the possibility for preventing tensile rupture of the axial bars by using improved deformed high-strength bars.

2.2 Outline of specimens

Fig. 1 shows the shape and reinforcement of specimens, and Table 1 shows the parameters of specimens in all the series. As shown in Table 1, different bars are used in different series, and in the specimens in the same series the buried depths of the piles are varied.

In Series 1, current PHC piles are used. In Series 2,

Table 1. List of specimens

Series	Specimen Numbers	Axial Bars (mm)	Axial Bars in Concrete Fill (mm)	Buried Depths of Piles (cm)
1	1-10	8-9.2 ϕ (Normal)	6-D22	10
	1-20			20
	1-30			30
	1-35			35
	1-40			40
	1-45			45
2	2-20	10-9.2 ϕ (Improved)	6-D22	20
	2-30			30
	2-45			45
3	3-10	12-7.4 ϕ (Normal)	6-D13	10
	3-20			20
	3-30			30
	3-45			45
4	4-10	8-9.2 ϕ (Normal)	6-D13	10
	4-20			20
	4-45			45

Axial Bars : Deformed high-strength bars
Axial Bars in Concrete Fill : Deformed bars

improved deformed high-strength bars are used as axial bars. Those bars have greater elongation ability (1.38 times) and lower yield stress (74.4%). In Series 3, normal deformed high-strength bars with smaller diameters are used as axial bars. In Series 4, only the section areas of the axial bars in the concrete fill are made less than those in Series 1. Fig. 3 shows an example of the pile section (Series 1).

2.3 Loading system

Fig. 4 shows the loading device. A cantilevered beam system was adopted as the loading system. The specimen was inverted, and horizontal force was loaded on the top of the pile via the loading jig. The loading of horizontal force was by cyclic reversed loading, and the maximum horizontal displacement at the loading point was 60mm (1/15 at slope angle).

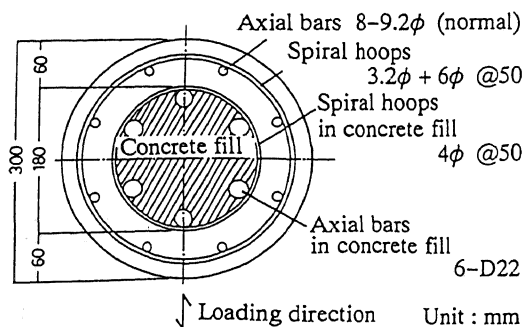


Figure 3. Details of pile section (Series 1)

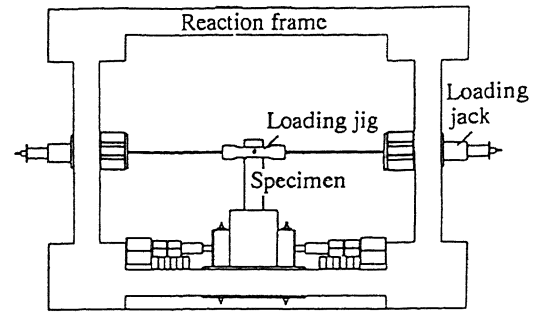


Figure 4. Loading device

3 RESULTS OF EXPERIMENTS AND REVIEW

Table 2 shows the experimental values of the maximum horizontal load (P_{max}), rupture forms, and the calculated values of the horizontal bearing load (P_{cal}). Reviews of the experiments are given in each series. The calculated values of the horizontal bearing load will be reviewed in Chapter 4.

3.1 Effects of buried depths of piles (Series 1)

3.1.1 Rupture forms and plastic deformability

Fig. 5 shows the relationship between the load of each specimen (P) and the displacement (δ) at the loading point.

In the specimen in which the pile was buried 10cm

Table 2. Results of experiments & calculations

Series	Specimen Numbers	$P_{max}(tf)$	Rupture Forms	$P_{cal}(tf)$	$\frac{P_{max}}{P_{cal}}$
1	1-10	12.1	F	12.7	0.95
	1-20	15.5	F	14.5	1.07
	1-30	16.0	F	16.3	0.98
	1-35	16.9	B	17.4	0.97
	1-40	17.4	B	17.8	0.98
	1-45	18.4	B	17.6	1.04
2	2-20	16.8	F	15.7	1.07
	2-30	18.0	F	17.4	1.03
	2-45	17.5	F	17.4	1.01
3	3-10	12.5	F	13.1	0.95
	3-20	16.0	F	15.3	1.05
	3-30	17.6	F	17.4	1.01
	3-45	16.4	B	17.5	0.94
4	4-10	6.9	F	6.3	1.09
	4-20	12.4	F	8.5	1.47
	4-45	13.4	B	12.2	1.10

P_{max} : Experimental values of maximum load

P_{cal} : Calculated values of bearing load (see Chap. 4)

Rupture Forms

F : Rupture did not occur.

B : Rupture of axial bars occurred.

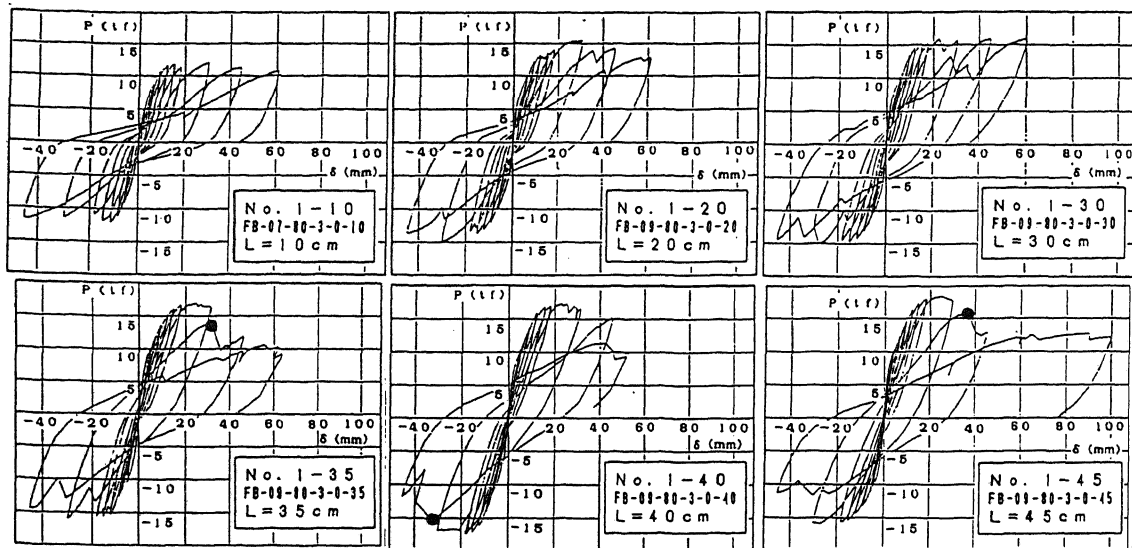


Figure 5. P- δ relationship (Series 1) (L : Buried depths of piles, ● : Rupture of axial bars)

deep, almost constant load was maintained even after the maximum load was reached, and the rupture of axial bars did not occur even at the point where displacement reached 60mm (1/15 at slope angle). Also the noise ascribable to anchorage bond slip was not heard, and the temporary decrease of load which is characteristic of anchorage bond slip was not noticed either. This can be explained by assuming that anchorage bond slip did occur, but the specimen adjusted to the deformation, maintaining the bond force at the time of anchorage bond slip.

In the specimens in which piles were buried 20cm and 30cm deep, the noises ascribable to anchorage bond slip and the temporary decreases of load were noticed repeatedly, but the rupture of axial bars did not occur even at the point of 60mm displacement, thus showing great plastic deformability.

In the specimen in which the pile was buried 35cm deep, axial bars slipped in the anchorage bond at the cycle of $\delta = -30$ mm, and at the cycle of $\delta = +45$ mm the rupture of axial bars occurred with loud noise. Also in the specimens with piles buried 40cm and 45cm deep, the rupture of axial bars occurred respectively at the cycles of $\delta = -45$ mm and $\delta = +45$ mm.

In the specimen with the pile buried 35cm deep or deeper, load decreased abruptly as soon as the rupture of the axial bars occurred. Subsequently, displacement was increased up to 60mm, but it only maintained the load after the decrease, and the maximum load before the decrease was not recovered.

Table 2 shows that the deeper the piles were buried, the more the maximum load increased. Since each specimen was the same, except that their buried depths were different, the change of the maximum load is considered to be due to the buried depth.

3.1.2 Maximum bond stress of axial bars

The experimental results of this series show that the minimum anchorage length of the axial bars (L_a) is between 35cm and 40cm. If $L_a=37.5$ cm, the maximum

bond stress is $\tau_a=90\text{kgf/cm}^2$ from Formula (2).

3.2 Effects of the yield stress of axial bars and their diameters (Series 2 and 3)

3.2.1 Rupture forms and plastic deformability

The results of the experiments in both series were similar to those of Series 1. However, when the piles were buried 45cm deep, although ruptures of axial bars occurred in the specimens of Series 1, 3 and 4, the rupture did not occur in the specimen of Series 2 even when displacement reached 60mm. In all the specimens the temporary decrease of load due to the anchorage bond slip of axial bars was not noticed and the axial bars were judged to be firmly anchored. It can be inferred, therefore, that the non-occurrence of axial bar rupture in Series 2 was due to the effect of the use of improved deformed high-strength bars, which have greater elongation ability after yielding.

3.2.2 Effects on flexural strength

Fig. 6 shows the relationship of the maximum loads (P_{\max}) and the buried depths of the piles (L) in the specimens in which axial bars slipped in the anchorage bond in comparison to Series 1. The total perimeters of the axial bars in Series 2 and 3 are respectively 1.25 and 1.21 times longer than those in Series 1.

Comparisons of the maximum loads of the specimens in which the piles were buried to the same depth show that the larger the total perimeter of axial bars was, the more the maximum load increased.

The comparison of Strength A and Strength B in Series 1 to 3 shows that the experimental values of Strength A (the maximum value of P_{\max} in each series in Table 2) are in approximately the same range of 17.6–18.4tf, and Strength B also corresponds since axial bars in the concrete fill are the same. Therefore, these experimental results confirm the anticipation of Chapter 2 (c) qualitatively.

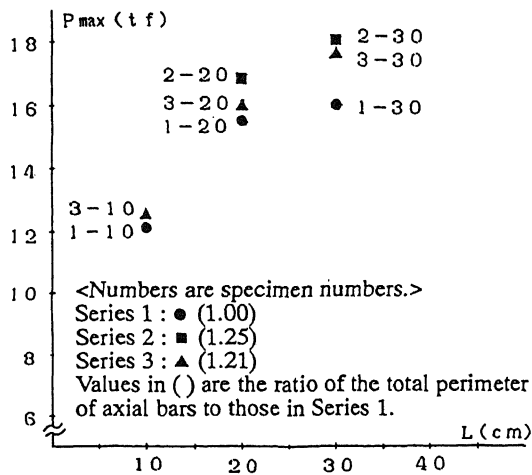


Figure 6. Relationship of maximum loads (P_{max}) and buried depths of piles (L) (Series 1, 2, & 3)

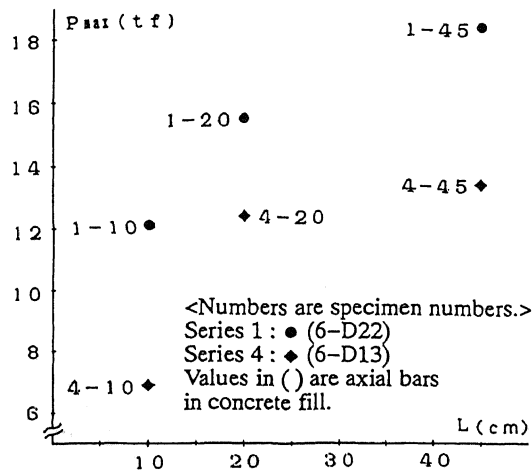


Figure 7. Relationship of maximum loads (P_{max}) and buried depths of piles (L) (Series 1 & 4)

3.3 Effects of axial bars in concrete fill (Series 4)

3.3.1 Rupture forms and plastic deformability

Review is omitted here since the experimental results in this series were about the same as those in Series 1, except that maximum loads decreased considerably because of decreasing the section areas of axial bars in the concrete fill.

3.3.2 Effects on flexural strength

Fig. 7 shows the relationship of the maximum loads (P_{max}) and the buried depths of piles (L) in the specimens with comparison to Series 1.

The comparison of the maximum loads in the specimens with the same buried depths of piles show that the maximum loads in this series with smaller section areas of axial bars in the concrete fill are lower

than those in Series 1, and the differences are about the same regardless of the buried depths of the piles. These results support the anticipation of Chapter 2 (a).

4 CALCULATION METHOD FOR FLEXURAL STRENGTH OF PHC PILE FOUNDATIONS

The effects of the anchorage bond slip of axial bars on the flexural strength of PHC pile foundations which were anticipated in Chapter 2 were confirmed qualitatively by the experiments in Chapter 3. In this chapter, a method for calculating the flexural strength of PHC pile foundations with consideration of the anchorage bond slip of axial bars is presented. This method will be verified quantitatively by applying it to all the specimens used in the experiments.

4.1 Assumptions for calculating flexural strength

The following are the assumptions for calculating the flexural strength of PHC pile foundations:

(a) The assumption that plane sections remain plane is taken for granted.

(b) The stress-strain relationship of concrete in the compression zone is described by the ϵ -function in Formula (3), and that in the tension zone is linear up to cleavage strength and the stress is zero there after.

$$\eta = -6.75 (e^{0.812 \cdot \xi} - e^{1.218 \cdot \xi}) \quad (3)$$

η : ratio of present stress and compressive strength
 ξ : ratio of present strain and the strain at compressive strength

(c) The stress-strain relationships of axial bar and axial bar in the concrete fill are completely elasto-plastic in both the compression and tension zones.

(d) The maximum bond stress of axial bars is $\tau_a = 90 \text{ kgf/cm}^2$ based on the experimental results in Series 1.

(e) The buried depth of the pile is equal to the anchorage length of the axial bars. The bond force of the axial bars is proportionate to the anchorage length. The minimum anchorage length is described by Formula (1).

(f) Axial bars slip in the anchorage bond when the buried depth is smaller than the minimum anchorage length, but the bond force at the time of anchorage bond slip is retained.

4.2 Method for calculating flexural strength with consideration of anchorage bond slip

The flexural strength of PHC pile foundations is determined by calculating the maximum value of the bending moment generated in the pile top section, while the curvature and the axial strain at the center of the section are varied so that the axial force generated in the section will be equal to the external axial force. In this calculation the anchorage bond slip of axial bars should be taken into consideration.

Formula (4) is obtained by transforming Formula (1).

$$\sigma_y = 4 \cdot \tau_a \cdot L_a / R \quad (4)$$

This means that Formula (5) is valid since the bond force of axial bars is proportionate to the buried depth of the piles.

$$\sigma' = \text{MIN} \{ \sigma_y, 4 \cdot \tau_a \cdot L / R \} \quad (5)$$

σ' : the apparent yield stress of axial bars with consideration of anchorage bond slip
 L : the buried depth of piles

When the yield stress of axial bars is modified by Formula (5) and their stress-strain relationship is assumed to be completely elasto-plastic, the bond force at the time of anchorage bond slip is retained and assumption (f) in the previous chapter is satisfied.

4.3 Comparison of experimental values and calculated values of flexural strength

Table 2 shows the bearing loads (Pcal) calculated with above calculation method of all the specimens used in the experiments in Chapter 3.

Table 2 shows that except in the case of Specimen 4-20, the values of Pmax/Pcal, that is, the ratio of the experimental value of the maximum load (Pmax) and the calculated value of the bearing load (Pcal) are in the range of 0.94 - 1.10 (average = 1.02), which means that the calculated values correspond well to the experimental values.

The explanation of the discrepancy between the calculated value and the experimental value of Specimen 4-20 has to be omitted here because of page limitations.

4.4 Comparison of strength lines and experimental values

Fig. 8 shows the strength lines shown in the concept figure of Fig. 2 which were calculated for each experimental series using the above method with comparison to the experimental results.

The strength line in each series is not an exact straight line as anticipated in Chapter 2, but appears slightly convex.

The experimental values (except Specimen 4-20) are more or less along the strength line in each series. Also Fig. 8 shows that the gradient of Series 2 in which the yield stress of axial bars is smaller than the specimens in Series 1 and the gradient of Series 3 in which the diameter of axial bars is smaller are greater than the gradient of Series 1, which supports the anticipation of Chapter 2 (b).

These reviews indicate that the method for calculating the flexural strength of PHC pile foundations presented in this chapter is valid.

5 CONCLUSION

The following are the items confirmed thus far in the experiments concerning PHC pile foundations by the proposed system:

(1) If the product of the ratio of spiral hoops and their yield stress is more than 9 times greater than current PHC piles, the shear failure and compressive rupture of piles can be prevented under any axial force and the

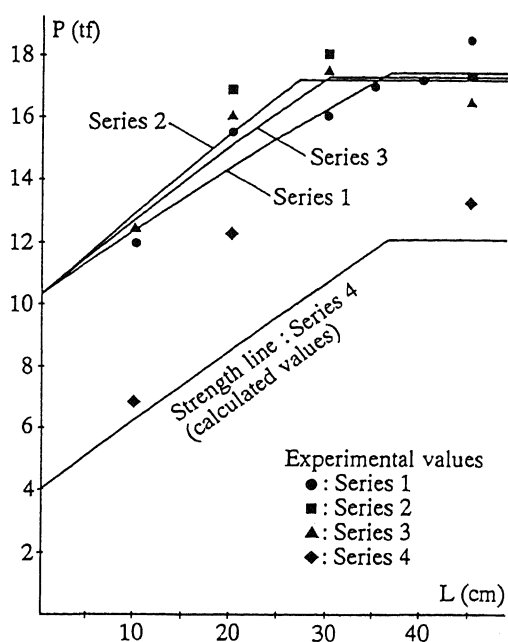


Figure 8. Comparison of strength lines and experimental values

plastic deformability of PHC pile foundations is greatly improved.

(2) The maximum bond stress of axial bars is $\tau_a = 90 \text{ kgf/cm}^2$.

(3) The minimum anchorage length of axial bars can be described by Formula (1), and is proportionate to their yield stress and diameter.

(4) If improved deformed high-strength bars are used as axial bars or if the buried depth of piles is smaller than the minimum anchorage length of axial bars, the rupture of axial bars under small axial force can be prevented. In the latter case, the temporary decrease of load due to the anchorage bond slip of the axial bars occurs, but in both cases, the plastic deformability of the PHC pile foundations is greatly improved.

(5) The flexural strength of PHC pile foundations under any axial force can be calculated by the presented method with consideration of the anchorage bond slip of axial bars. The calculated values by this method correspond well to the experimental values.

(6) The flexural strength of PHC pile foundations can be adjusted by the quantity of axial bars in the concrete fill, and the strength is stronger than in the case of the PHC piles without axial bars in the concrete fill.

REFERENCES

- Kokusho, S. et al. 1984. Experimental study on plastic deformability of high strength prestressed concrete piles under axial and lateral forces. Proc. 8th WCEE: Vol. 3 609-616
- Kokusho, S. et al. 1988. Improvement of deformability of high-strength prestressed concrete piles. Proc. 9th WCEE: Vol. 3 611-615